as well (see Supplementary Table 2 and Supplementary Methods). Tycho G has significant proper motion toward lower Galactic latitude: $\mu_b = -6.11 \pm 1.34\,\mathrm{mas\,yr^{-1}}$ (the proper motion along longitude is small, $\mu_l = -2.6 \pm 1.34\,\mathrm{mas\,yr^{-1}}$). The proper motion in Galactic latitude implies that this star is an outlier in proper motion as well, with a derived tangential velocity of $94 \pm 27\,\mathrm{km\,s^{-1}}$ (a $24\,\mathrm{km\,s^{-1}}$ systematic error was added, resulting from a $1.7\,\mathrm{mas\,yr^{1}}$ uncertainty in the reference frame solution of the images). The other stars do not show such coincidence in distance and high tangential velocity. The modulus of the velocity vector has a value of $136\,\mathrm{km\,s^{-1}}$, which is a factor of over 3 larger than the mean velocity value at 3 kpc.

If Tycho G is the companion star as suggested by its kinematics, the explosion centre should have been 2.6 arcsec north of the current location of this star on the basis of its velocity. The peculiar velocity would correspond to the peculiar velocities expected from the disruption of a white dwarf plus subgiant/main-sequence system[9,10] of roughly a solar mass. The system would have resembled the recurrent nova U Scorpii (see Supplementary Note 2). The excess velocity corresponds to a period of about 2–7 days, for a system made of a white dwarf close to the Chandrasekhar mass plus a companion of roughly a solar mass at the moment of the explosion.

Several paths lead to this star as the likely donor star of SN 1572: its high peculiar velocity (both radial and tangential velocities), the distance in the range of SN 1572, and its type, which fits the post-explosion profile of a type Ia supernova companion, as the position of this star in the Hertzsprung–Russell diagram is also untypical for a standard subgiant. The lower limit to the metallicity obtained from the spectral fits is $[\mathrm{M/H}] > -0.5$ (see Fig 3 and Supplementary Fig. 1), which excludes its belonging to the Galactic halo population as an alternative explanation of its high velocity. Spectra taken at five different epochs also exclude its being a single-lined spectroscopic binary. If our candidate is the companion star, its overall characteristics imply that the supernova explosion affected the companion mainly through the kinematics. Our search for the binary companion of Tycho's supernova has excluded giant stars. It has also shown the absence of blue or highly luminous objects as post-explosion companion stars. A star very similar to the Sun but of a slightly more evolved type is here suggested as the likely mass donor that triggered the explosion of SN 1572. That would connect the explosion to the family of cataclysmic variables. □

Received 14 June; accepted 8 September 2004; doi:10.1038/nature03006.

1. Branch, D., Livio, M., Yungelson, L. R., Boffi, F. & Baron, E. In search of the progenitors of Type Ia Supernovae. *Publ. Astron. Soc. Pacif.* **107,** 1019–1029 (1995).
2. Ruiz-Lapuente, P., Canal, R. & Burkert, A. in *Thermonuclear Supernovae* (eds Ruiz-Lapuente, P., Canal, R. & Isern, J.) 205–230 (Kluwer Academic, Dordrecht, 1997).
3. Livio, M. in *Type Ia Supernovae: Theory and Cosmology* (eds Niemeyer, J. C. & Truran, J. W.) 33–48 (Cambridge Univ. Press, Cambridge, 2000).
4. Brahe, T. Astronomiae Instauratae Progymnasmata. In *Opera Omnia* Vol. 2 (ed. Dreyer, I. L. E.) 307 (Swets & Zeitlinger, Amsterdam, 1972) (1603).
5. Baade, W. B Cassiopeiae as a supernova of Type I. *Astrophys. J.* **102,** 309–317 (1945).
6. Baldwin, J. E. & Edge, D. O. Radio emission from the remnants of the supernovae of 1572 and 1604. *Observatory* **77,** 139–143 (1957).
7. Hughes, J. P. *et al.* ASCA observations of the Large Magellanic Cloud supernova remnant sample: Typing supernovae from their remnants. *Astrophys. J.* **444,** L81–L84 (1995).
8. Canal, R., Méndez, J. & Ruiz-Lapuente, P. Identification of the companion stars of Type Ia supernovae. *Astrophys. J.* **550,** L53–L56 (2001).
9. Ruiz-Lapuente, P. Tycho Brahe's supernova: light from centuries past. *Astrophys. J.* **612,** 357–363 (2004).
10. Ruiz-Lapuente, P. *et al.* in *From Twilight to Highlight: the Physics of Supernovae* (eds Hillebrandt, W. & Leibundgut, B.) 140–147 (Springer, Berlin, 2003).
11. Hachisu, I., Kato, M. & Nomoto, K. A new model for progenitor systems of Type Ia supernovae. *Astrophys. J.* **470,** L97–L100 (1996).
12. Li, X.-D. & van den Heuvel, E. P. J. Evolution of white dwarf binaries: supersoft X-ray sources and progenitors of type Ia supernovae. *Astron. Astrophys.* **322,** L9–L12 (1997).
13. Livio, M. & Truran, J. W. Type I supernovae and accretion-induced collapses from cataclysmic variables? *Astrophys. J.* **389,** 695–703 (1992).
14. Marietta, E., Burrows, A. & Fryxell, B. Type Ia supernova explosions in binary systems: the impact on the secondary star and its consequences. *Astrophys. J. Suppl.* **128,** 615–650 (2000).
15. Podsiadlowski, P. On the evolution and appearance of a surviving companion after a Type Ia supernova explosion. Preprint at ⟨http://arxiv.org/astro-ph/0303660⟩ (2003).
16. Lejeune, Th., Cuisinier, F. & Buser, R. A standard stellar library for evolutionary synthesis. *Astron. Astrophys. Suppl. Ser.* **125,** 229–246 (1997).
17. Brand, J. & Blitz, L. The velocity field of the outer Galaxy. *Astron. Astrophys.* **275,** 67–90 (1993).
18. Binney, J. & Merrifield, M. *Galactic Astronomy* (Princeton Univ. Press, Princeton, 1998).
19. Dehnen, W. & Binney, J. Local stellar kinematics from *Hipparcos* data. *Mon. Not. R. Astron. Soc.* **298,** 387–394 (1998).
20. Ruiz-Lapuente, P. Probing the nature of Type Ia SNa through HST astrometry. ⟨http://archive.stsci.edu/cgi-bin/proposal_search?mission = hst&id = 9729⟩ (2003).
21. Ruiz-Lapuente, P. in *Proc. Conf. Astronomy as a Model for the Sciences in Early Modern Times, Munich, 21–23 March 2003* (eds Fritscher, B. & Kühne, A.) (Erwin Rauner, Augsberg, in the press).
22. Hughes, J. P. The expansion of the X-ray remnant of Tycho's supernova (SN 1572). *Astrophys. J.* **545,** L53–L56 (2000).
23. Decourchelle, A. *et al.* XMM-Newton observation of the Tycho supernova remnant. *Astron. Astrophys.* **365,** L218–L224 (2001).
24. ⟨http://cxc.harvard.edu/cda/⟩
25. Anders, E. & Grevesse, N. Abundances of the elements—meteoritic and solar. *Geochim. Cosmochim. Acta* **53,** 197–214 (1989).
26. Kurucz, R. L. ATLAS9 Stellar Atmospheres Programs, Grids of Model Atmospheres and Line Data [CD-ROM]. (Smithsonian Astrophysical Observatory, Cambridge, MA, 1993).
27. Gustaffson, B., Bell, R. A., Eriksson, K. & Nordlund, Å. A grid of model atmospheres for metal-deficient giant stars. *Astron. Astrophys.* **42,** 407–432 (1975).
28. Schmidt-Kaler, Th. in *Landolt-Börnstein, New Ser. VI*, Vol. 2b (ed. Hellwege, K.-H.) 1–34 (Springer, Berlin, 1982).

Supplementary Information accompanies the paper on **www.nature.com/nature**.

Acknowledgements P.R.L. thanks C. Ruiz Ogara for giving her the spirit to complete this survey. We thank the support staff at the European Northern Observatory at La Palma for their assistance throughout this project, as well as the support staff at the W. M. Keck Observatory and NASA/ESA Hubble Space Telescope. We express our special gratitude to C. Abia, F. Figueras, C. Guirao, R. Mignani and J. Torra for diverse consultations. This work has been supported by DURSI, DGYCIT (to P.R.L., J.M. and R.C.), PPARC (to J.M. and S.J.S.) and by NSF (to A.V.F., R.C., R.J.F. and R.L.K.).

Competing interests statement The authors declare that they have no competing financial interests.

Correspondence and requests should be addressed to P.R.L. (pilar@am.ub.es).

Recent ice-rich deposits formed at high latitudes on Mars by sublimation of unstable equatorial ice during low obliquity

Benjamin Levrard[1]*, François Forget[2], Franck Montmessin[3] & Jacques Laskar[1]

[1]*Astronomie et Systèmes Dynamiques, IMC-CNRS UMR8028, 77 Avenue Denfert-Rochereau, 75014 Paris, France*
[2]*Laboratoire de Météorologie Dynamique, Université Paris VI, 4 Place Jussieu, 75005 Paris, France*
[3]*Space Science Division MS 245-3, NASA/Ames Research Center, Moffett Field, California 94035, USA*

* Present address: Laboratoire de Planétologie et télédétection, UMR 5570, UCBL-ENS Lyon, 43 boulevard du 11 novembre 1918, 69622 Villeurbanne, France

Observations from the gamma-ray spectrometer instrument suite on the Mars Odyssey spacecraft have been interpreted as indicating the presence of vast reservoirs of near-surface ice in high latitudes of both martian hemispheres[1–5]. Ice concentrations are estimated to range from 70 per cent at 60° latitude to 100 per cent near the poles, possibly overlain by a few centimetres of ice-free material in most places[4]. This result is supported by morphological evidence of metres-thick layered deposits that are rich in water-ice[6–9] and periglacial-like features[10,11] found only at high latitudes. Diffusive exchange of water between the pore space of the regolith and the atmosphere has been proposed to explain this distribution[12], but such a degree of concentration is

difficult to accommodate with such processes[9,13,14]. Alternatively, there are suggestions that ice-rich deposits form by transport of ice from polar reservoirs and direct redeposition in high latitudes during periods of higher obliquity[9,13], but these results have been difficult to reproduce with other models. Here we propose instead that, during periods of low obliquity (less than 25°), high-latitude ice deposits form in both hemispheres by direct deposition of ice, as a result of sublimation from an equatorial ice reservoir that formed earlier, during a prolonged high-obliquity excursion. Using the ice accumulation rates estimated from global climate model simulations we show that, over the past ten million years, large variations of Mars' obliquity have allowed the formation of such metres-thick, sedimentary layered deposits in high latitude and polar regions.

On Earth, quasi-periodic variations in orbital (eccentricity, longitude of perihelion from the moving equinox L_p) and spin axis parameters are implicated in significant climatic changes in the past million years (Myr)[15]. Oscillations between glacial and interglacial periods are characterized by a transfer of large amounts of water between polar ice sheets and oceans. Similarly, astronomical forcing and consequent changes in seasonal and global insolation are presumed to cause large-scale redistribution and cycling of volatiles at Mars' surface over timescales of $\sim 10^4$–10^6 years. In particular, previous simplified and full three-dimensional (3D) climate models have predicted that at much higher obliquities (>40°), polar ice may sublime rapidly and be redeposited in the tropics[13,16–19].

The variations of obliquity and orbital parameters of Mars are strongly chaotic[20,21]. Nevertheless, our knowledge of the present rotational state of Mars is sufficient to give a reliable solution of their evolution for the past 10 Myr (refs 22, 23). Over this interval, Mars' obliquity is characterized by a marked transition around 4 Myr ago between a high-mean-obliquity regime of $\sim 35 \pm 10°$ and a more recent low-obliquity regime of $\sim 25 \pm 10°$ (Fig. 1), while its eccentricity has varied between 0 and ~0.12 with a dominant ~2.4-Myr modulating period. Here, we use the martian global climate model (GCM)[24,25] of the Laboratoire de Météorologie Dynamique (LMD) to investigate the evolution of surface ice deposits across the large obliquity changes of this transition. We used a horizontal resolution of 7.5° in longitude and 5.625° in latitude and 25 vertical levels. The model includes a full description of exchange between surface ice and atmospheric water, transport and turbulent mixing of water in the atmosphere and cloud formation[25,26]. The radiative effects of water vapour and clouds as well as the exchanges of water vapour with the subsurface are not included. The surface albedo is set to 0.4 when an ice layer thicker than 5 μm is present, enabling an ice-albedo feedback process. The surface thermal inertia is not modified, however. Control simulations of seasonal water cycle for the present-day orbital parameters provide latitudinal distributions of atmospheric vapour and clouds in very good agreement with TES spectrometer observations[26,27].

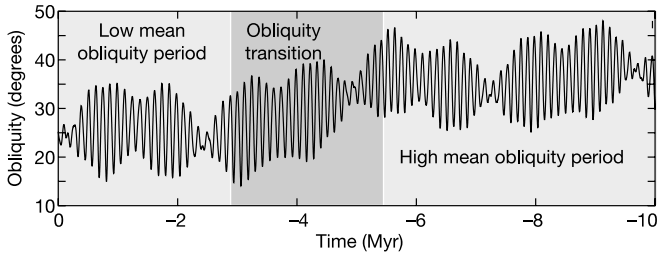

Figure 1 Evolution of the martian obliquity in the past 10 Myr. Characteristic periods are indicated: high- and low-mean obliquity periods in pale grey, obliquity transition in dark grey; after Laskar *et al.*[23]. The main obliquity periodicity is about 120,000 earth years.

In a first set of simulations, we investigated the global stability of the northern ice cap for obliquity values ranging from the present value (25.19°) to 45° in 5° steps. In each case, the model is spun up from dry initial conditions with a northern residual ice cap as the only initial water source and then run until the atmosphere comes to an interannually repeatable state. The cap is 'unstable' (it undergoes a net loss) when the water lost in summer is not transported back during the rest of the year. To first order, we found that the net amount of water sublimed from the cap (per unit surface area) and transported to nonpolar regions depends mainly on the summer polar insolation, which is a sensitive function of both obliquity and orbital parameters.

For circular orbits, the cap is unstable for obliquities higher than 35° and the corresponding annual loss rates are 6.5, 27.8 and 65.0 mm per martian year for obliquities ranging from 35 to 45°. However, for an orbit with the current Mars eccentricity (0.0934), and with a perihelion coincident with the northern summer solstice ($L_p = 90°$), thus maximizing the summer polar insolation, the northern cap already becomes unstable at 30° obliquity. Annual water loss rates then reach 5.0, 26.5, 80.2 and 218 mm per martian year for obliquities ranging from 30 to 45°, respectively. Conversely, when the northern summer solstice corresponds to the aphelion ($L_p = 270°$), obliquities of 40° and higher are required to obtain an unstable cap and the annual loss rates are 7.2 and 21.6 mm yr^{-1} for 40° and 45° values, respectively. Thus, in our model, there is a critical obliquity between 35 and 40°, above which the stability of the north polar cap is lost whatever the values of the orbital parameters, in agreement with ref. 13.

In all these cases, the LMD model predicts substantial ice deposition in the tropics, in agreement with previous GCM studies[13,18]. However, unlike in ref. 13 no accumulation of stable ice was ever found in the mid- and high latitudes for any obliquities when assuming a polar source. The NASA Ames GCM also does not reproduce this behaviour (R. M. Haberle, personal communication).

In our simulations, when the polar cap is unstable, ice accumulation occurs in the high topography areas of Tharsis Montes and Olympus Mons where the saturation state of the atmosphere becomes the highest (Fig. 2). Ice precipitation is favoured by adiabatic cooling and upwelling of atmospheric water on the windward slopes. For a typical circular orbit, net ice accumulation rates may reach ~15 mm per martian year at 35°, 30 mm yr^{-1} at 40°

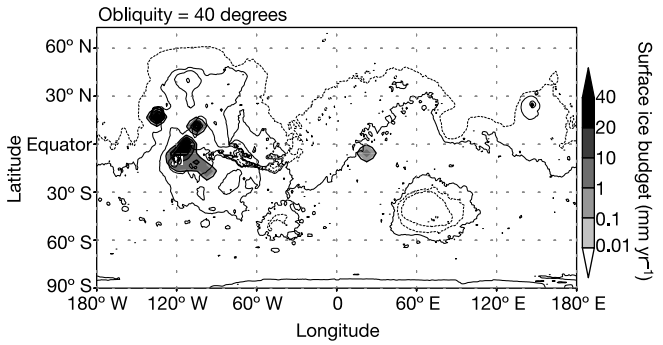

Figure 2 Surface water ice budget (in millimetres per martian year) for a 40° obliquity during simulation year 11, with superimposed MOLA topography. The eccentricity is set to zero. Main accumulation regions are located on Tharsis Rise (around Arsia, Pavonis and Ascraeus Montes) and Olympus Mons. Minor accumulation (~1 mm per martian year) occurs near the equatorial Schiaparelli basin impact. For other obliquities and/or orbital parameters leading to a vanishing northern water ice cap, the locations of stable surface ice are similar and also concentrated on the Tharsis area and Olympus Mons, but with local variations of ice accumulation rates. Climate simulations performed with higher resolution (3.75° in longitude and 5.625° in latitude) result in more localized ice sheets on Tharsis Montes and Olympus Mons.

and 60 mm yr^{-1} at 45° on some of Tharsis Montes. We thus believe that, during the mean high-obliquity regime (~5–10 Myr ago), and unless a dust lag inhibited polar sublimation, a few obliquity cycles may have been sufficient to empty the polar reservoirs and form massive glaciers ~3 km thick or more on the Tharsis Montes and Olympus Mons, depending on the amount of polar water available. This could explain the presence of fan-shaped deposits interpreted as remnant traces of 'cold-based' glaciers on their western flanks[28,29].

When the obliquity dropped below the critical value, the equatorial ice reservoirs began to sublime and lose water, leading to the redistribution of ice to other areas on the surface of Mars. To investigate where the ice may have gone under these circumstances, we performed climate simulations for obliquities 30, 25.19, 20 and 15°, all starting with an equatorial ice reservoir as the only source of water on the surface. We tested various sizes and locations of these reservoirs and various initial atmospheric water contents. These simulations yielded similar results. Below, we discuss results from simulations performed assuming an initial dry atmosphere and an ice reservoir on Tharsis Montes (Fig. 3), for a circular orbit.

The annual surface ice budgets obtained from these simulations (Fig. 3) show that the ice returns to the high-latitude and polar areas of both hemispheres, but that the extent of the ice distribution is sensitive to obliquity. At 30° obliquity, the ice accumulates only in the northern polar areas. Because the eccentricity here is set to zero, we attributed this asymmetry to biasing of the general circulation by the topography differences between the two hemispheres[30]. At the current obliquity (~25.2°), ice covers most areas north of 65° N and begins to accumulate near the south pole. Finally, at 20° and 15° obliquities, large-scale ice accumulation is observed poleward of ~60° in both hemispheres with some excursions into the mid-latitude regions (~30–60° S) of the Southern hemisphere. Despite its zonal dependence, the boundaries of the global ice distribution exhibit significant coincidence with the near-surface ice distribution inferred from GRS data[1–5] and latitude-dependent ice-rich deposits from MOLA and MOC data[29], especially in the northern hemisphere.

The fact that the surface ice becomes stable and accumulates at subpolar latitudes for obliquity equal to or lower than today's when an equatorial source is present is an unavoidable consequence of the high water-vapour content of the atmosphere under such conditions. Currently on Mars at 25.19° obliquity, surface ice also accumulates in autumn, winter and early spring at 60–75° latitude. However, this layer of ice always remains thinner than 0.5 mm on average (in our current Mars GCM simulation) and quickly sublimes after mid-spring. When an equatorial source is present, much more water vapour is transported to the high latitudes and the amount of ice that accumulates during autumn, winter and early spring can reach several millimetres above 65° N. This is more than the amount that can sublime in late spring (~1–2 mm). At obliquity lower than today's, the water content of the global atmosphere is about the same as at the current obliquity, but the late spring and summer ice sublimation is lower because of the reduced insolation.

Ice deposition rates in high and polar latitudes appear to be weakly sensitive to the obliquity value (Fig. 3). Above 65° N, these rates remain close to ~2 mm per martian year between 25 to 15° obliquity, and are slightly lower in the southern hemisphere. With such low rates, it is likely that a significant amount of dust was incorporated in the icy deposits if the atmosphere was as dusty as today's. Nevertheless, assuming a steady accumulation of 2 mm per martian year, we can estimate that much more than 10 m of ice-rich material should have accumulated during each obliquity cycle when

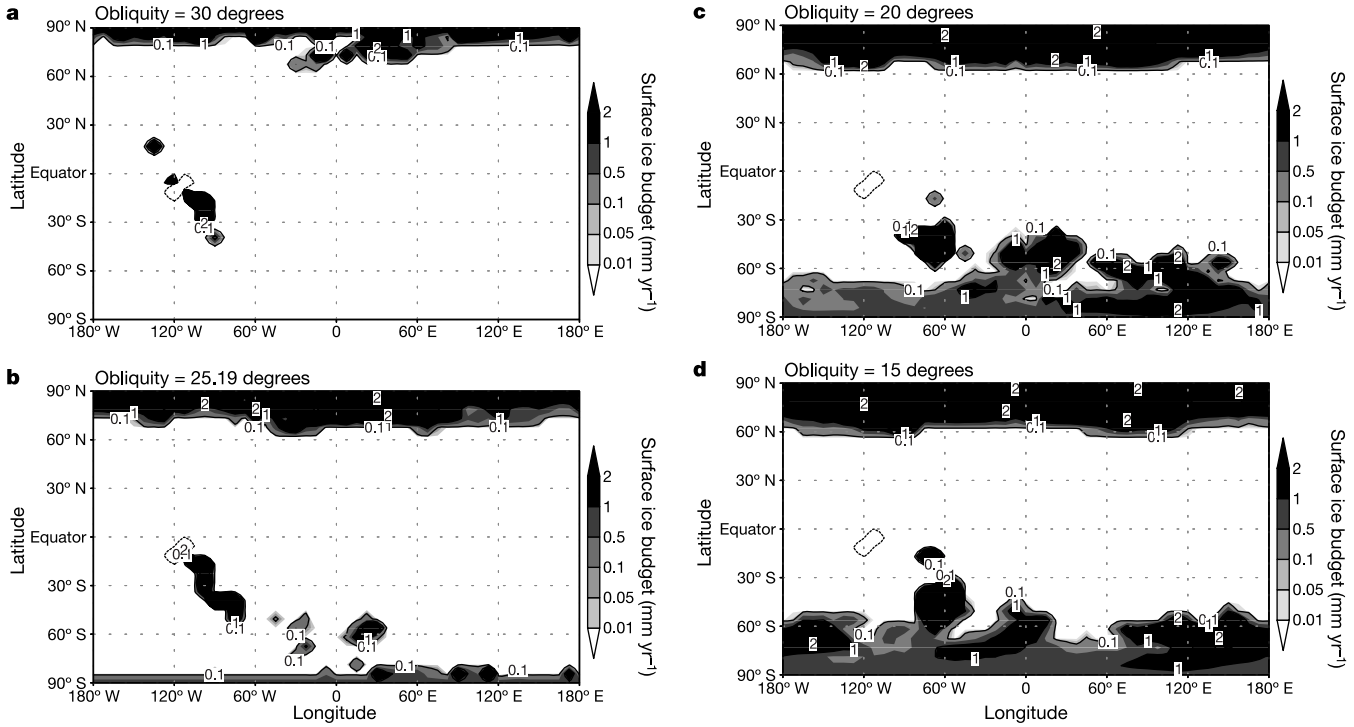

Figure 3 Surface water ice budget in mm per martian year after ten years of simulation for various obliquities, and with an example of equatorial ice reservoir situated around Arsia and Pavonis Montes. **a**, 30°; **b**, present obliquity 25.19°; **c**, 20°; **d**, 15°. Its boundaries are indicated by a thick solid line. We assume dry initial conditions and the equatorial reservoir as the only water source. The eccentricity is set to zero. In that case, the critical obliquity for the northern polar cap stability is between 30 and 35°. At 25.19° and 30° obliquities, local accumulation occurs in tropical zones around the equatorial source, which depends on the extent and the location of the source. At high latitudes, ice accumulation is more uniformly distributed in longitude and latitude in the northern than in the southern hemisphere. Typical accumulation rates (~2 mm per martian year) are an order of magnitude lower than the ice loss rates at high obliquity, suggesting that pure polar ice deposits may not survive during the high mean obliquity regime (~5–10 Myr ago).

the obliquity was below 25°, because each of these episodes lasted about 60,000 years. A significant part of this ice probably sublimed during the other half of the obliquity cycle with obliquity above 30°. However, as suggested by refs 13 and 14, the upper part of the ice layers sublimated, but probably left behind a dry slab layer that protected deeper ice deposits from further sublimation. If this is accurate, then each obliquity cycle created at least one distinct layer which may still be present below the surface of Mars.

However, this process supposes that an equatorial ice reservoir remained present during periods of low obliquity. To test this hypothesis, we analysed the ice loss rates of individual equatorial sources at low obliquity for initial ice distributions issued from high-obliquity simulation distributions (Fig. 2). We found minimal loss rates of ~1.0, 10, 15 and 20 mm per martian year at 30, 25.19, 20 and 15° obliquity, respectively. Integrating a simple deposition/sublimation history over the obliquity cycles of the obliquity transition shows that a 3-km-thick equatorial ice source may have survived throughout the whole transition until ~3 Myr ago.

Once the equatorial sources were exhausted, what finally happened to the high-latitude ice deposits? To address this issue, we performed simulations starting with the initial ice inventory of the previous simulations (as on Fig. 3) but without the equatorial source. We found that the edges of the mid- and high-latitude deposits become unstable and are redeposited poleward. Further simulations indicate that the surface ice slowly retreats to the pole. There again, it is likely that in reality only the upper ice sublimed and that a significant part of the layer remained under a protecting lag deposit, the one that we still see today at the surface of Mars.

Over longer timescales (~10^9 years), the 'chaotic diffusion' of Mars' obliquity shows that periods of high obliquity (>40°) are statistically the most probable situation[23], suggesting that our mechanism could have acted throughout martian geological history. In this context, it is possible that the near-surface ice detected by Mars Odyssey is only the upper layer of a much deeper ice reservoir. Future MARSIS and SHARAD sounding investigations aboard Mars Express and the Mars Reconnaissance Orbiter may provide important constraints on these reservoirs. □

Received 8 April; accepted 17 September 2004; doi:10.1038/nature03055.

1. Mitrofanov, I. *et al.* Maps of subsurface hydrogen from the high energy neutron detector, Mars Odyssey. *Science* **297,** 78–81 (2002).
2. Boynton, W. V. *et al.* Distribution of hydrogen in the near surface of Mars: evidence for subsurface ice deposits. *Science* **297,** 81–85 (2002).
3. Feldman, W. C. *et al.* Global distribution of neutrons from Mars. *Science* **297,** 75–78 (2002).
4. Boynton, W. V. *et al.* Constraints on the distribution of hydrogen in the polar regions of Mars and implications for ice formation processes. *AGU Fall Meeting Abstr.* Abst. P32B-05 (2003).
5. Feldman, W. C. *et al.* The global distribution of near-surface hydrogen on Mars. *J. Geophys. Res.* **109** (E6), doi:10.1029/2003JE002160 (2004).
6. Mustard, J. F., Cooper, C. D. & Rifkin, M. K. Evidence for recent climate change on Mars from the identification of youthful near-surface ground ice. *Nature* **412,** 411–414 (2001).
7. Kreslavsky, M. A. & Head, J. W. Kilometre-scale roughness of Mars: Results from MOLA data analysis. *J. Geophys. Res.* **105,** 26695–26711 (2000).
8. Kreslavsky, M. A. & Head, J. W. Nature and evolution of young latitude-dependent water-ice rich mantle. *Geophys. Res. Lett.* **29,** doi:10.1029/2002GL015392 (2002).
9. Head, J. W., Mustard, J. F., Kreslavsky, M. A., Milliken, R. E. & Marchant, D. R. Recent ice ages on Mars. *Nature* **426,** 797–802 (2003).
10. Mangold, N., Maurice, S., Feldman, W. C., Costard, F. & Forget, F. Geographical relationships between small scale polygons and ground ice distribution from neutron spectrometer on Mars. *Third Mars Polar Sci. Conf.* Abst. 8043 (2003).
11. Milliken, R. E. *et al.* Viscous flow features on the surface of Mars. *J. Geophys. Res.* **108** (E6), doi:10.1029/2002JE002005 (2003).
12. Mellon, M. T., Feldman, W. C. & Prettyman, T. H. The presence and stability of ground ice in the Southern hemisphere of Mars. *Icarus* **169,** 324–340 (2004).
13. Mischna, M. A., Richardson, M. I., Wilson, R. J. & McCleese, D. J. On the orbital forcing of Martian water and CO_2 cycles: A general circulation model study with simplified volatile schemes. *J. Geophys. Res.* **108** (E6), doi:10.1029/2003JE002051 (2003).
14. Mischna, M. A., McCleese, D. J., Richardson, M. I., Vasavada, A. R. & Wilson, R. J. Volatile cycling and layering on Mars: Observations, theory and modeling. *6th Int. Mars Conf.* Abst. 3145 (2003).
15. Hays, J. D., Imbrie, J. & Shackleton, N. J. Variations of the Earth's Orbit: pacemaker of the ice ages. *Science* **194,** 1121–1132 (1976).
16. Jakosky, B. M. & Carr, M. H. Possible precipitation of ice at low latitudes of Mars during periods of high obliquity. *Nature* **315,** 559–561 (1985).
17. Jakosky, B. M., Henderson, B. G. & Mellon, M. T. Chaotic obliquity and the nature of the Martian climate. *J. Geophys. Res.* **100,** 1579–1584 (1995).
18. Haberle, R. M. *et al.* The Martian water cycle at high obliquity. *Lunar Planet. Sci. Conf.* **XXXI** Abst. 1509 (2000).
19. Richardson, M. I. & Wilson, R. J. Investigation of the nature and stability of the Martian seasonal water cycle with a general circulation model. *J. Geophys. Res.* **107** (E5), doi:10.1029/2001JE001536 (2002).
20. Laskar, J. & Robutel, P. The chaotic obliquity of the planets. *Nature* **361,** 608–612 (1993).
21. Touma, J. & Wisdom, J. The chaotic obliquity of Mars. *Science* **259,** 1294–1297 (1993).
22. Laskar, J., Levrard, B. & Mustard, J. F. Orbital forcing of the martian polar layered deposits. *Nature* **419,** 375–377 (2002).
23. Laskar, J. *et al.* Long term evolution and chaotic diffusion of the insolation quantities of Mars. *Icarus* **170,** 343–364 (2004).
24. Hourdin, F., Forget, F. & Talagrand, O. Meteorological variability and the annual surface pressure cycle on Mars. *J. Atmos. Sci.* **50,** 3625–3640 (1993).
25. Forget, F. *et al.* Improved General Circulation Models of the Martian atmosphere from the surface to above 80 km. *J. Geophys. Res.* **104,** 24155–24176 (1999).
26. Montmessin, F., Forget, F., Rannou, P., Cabane, M. & Haberle, R. M. Origin and role of water ice clouds in the Martian water cycle as inferred from a general circulation model. *J. Geophys. Res.* **109** (E10), doi:10.1029/2004JE002284 (2004).
27. Smith, M. D. The annual cycle of water vapor on Mars as observed by the Thermal Emission Spectrometer. *J. Geophys. Res.* **107** (E6), 10.1029/2001JE001522 (2002).
28. Head, J. W. & Marchant, D. R. Cold-based moutain glaciers on Mars: Western Arsia Mons. *Geology* **31,** 641–644 (2003).
29. Shean, D. E., Head, J. W., Fastook, J. L. & Marchant, D. R. Tharsis Montes cold-based glaciers: Observations and constraints for modeling and preliminary results. *Lunar Planet. Sci. Conf.* **XXXV** Abst. 1428 (2004).
30. Richardson, M. I. & Wilson, R. J. A topographically forced asymmetry in the martian circulation and climate. *Nature* **416,** 298–301 (2002).

Acknowledgements We acknowledge R. M. Haberle and G. L. Tyler for useful discussions and comments. This work was supported by the CNRS-PNP programme.

Competing interests statement The authors declare that they have no competing financial interests.

Correspondence and requests for materials should be addressed to B.L. (blevrard@imcce.fr).

Continuous generation of single photons with controlled waveform in an ion-trap cavity system

Matthias Keller[1], Birgit Lange[1], Kazuhiro Hayasaka[2], Wolfgang Lange[1] & Herbert Walther[1,3]

[1]*Max-Planck-Institut für Quantenoptik, Hans-Kopfermann-Strasse 1, 85748 Garching, Germany*
[2]*National Institute of Information and Communications Technology, 588-2 Iwaoka, Nishi-ku, Kobe 651-2492, Japan*
[3]*Sektion Physik der Universität München, Am Coulombwall 1, 85748 Garching, Germany*

The controlled production of single photons is of fundamental and practical interest; they represent the lowest excited quantum states of the radiation field, and have applications in quantum cryptography[1] and quantum information processing[2]. Common approaches use the fluorescence of single ions[3], single molecules[4,5], colour centres[6,7] and semiconductor quantum dots[8–12]. However, the lack of control over such irreversible emission processes precludes the use of these sources in applications (such as quantum networks[13]) that require coherent exchange of quantum states between atoms and photons. The necessary control may be achieved in principle in cavity quantum electrodynamics. Although this approach has been used for the production of single photons from atoms[14–16], such experiments are compromised by limited trapping times, fluctuating atom–field coupling and multi-atom effects. Here we demonstrate a single-photon source based on a strongly localized single ion in an optical cavity. The ion is optimally coupled to a well-defined field mode, resulting in the generation of single-photon pulses with precisely defined shape and timing. We have confirmed the